ELSEVIER

# Electrokinetics in extremely bimodal suspensions ☆

M.L. Jiménez [a,*], F.J. Arroyo [b], A.V. Delgado [a], F. Mantegazza [c], T. Bellini [d], R. Rica [a]

[a] Department of Applied Physics, Faculty of Science, University of Granada, Spain
[b] Department of Physics, Faculty of Experimental Science, University of Jaén, Spain
[c] DIMESAB, Universita' degli Studi di Milano-Bicocca, Monza (MI), Italia
[d] Dipartimento di Chimica, Biochimica e Biotecnologie per la Medicina, Università di Milano, Segrate (MI), Italy

## Abstract

Prompted by the results obtained by Mantegazza et al. [Nature Physics 1 (2005) 103], where the electric birefringence of suspensions of elongated particles was strikingly affected by the presence of a sea of very small (size ratio lower than 10:1) colloidal spheres, we have undertaken an investigation of other electrokinetic phenomena in suspensions containing various relative concentrations of large (Teflon or polystyrene latex) and small (nanometer-sized silica spheres) colloids. We have determined the quantities that might be greatly affected by the size distribution of the particles, mainly in the presence of ac electric fields, since the response of the suspensions will show very characteristic relaxations, dominated in principle by the size of the particles. In this work, we report on measurements of the dielectric dispersion of mixed particles as a function of the concentration, ionic strength, and field frequency. The results indicate that the response is not just a simple combination of those obtained with suspensions of the individual particles, and in fact the presence of even small amounts of the small particles affects considerably the frequency response of the suspensions.
© 2007 Elsevier Inc. All rights reserved.

Keywords: Electric permittivity; Bimodal suspensions; Concentrated suspensions

## 1. Introduction

During the past years, a number of phenomena have been described that are a consequence of interactions between particles in colloidal suspensions, such as electrically or magnetically induced structures [1–6] or phase separation in bidisperse systems [7–9]. In particular, it has long been reported that some dispersed systems exhibit intriguing anomalous electroorientation manifested in negative electric birefringence [10–14]. But all these phenomena disappear for dilute suspensions, for which the interactions between particles can usually be neglected and only single-particle effects are expected to be measured.

However, electrokinetic and related phenomena of dilute systems are not completely understood. For instance, it has been experimentally shown that the usual parallel orientation of elongated particles under the action of an electric field is dramatically affected by the presence of small quantities of nanoscale charged particles [15]. Electric birefringence spectroscopy measurements demonstrate that the anomalous orientation is affected by both the particle charge and medium conductivity. This phenomenon, only partially understood up to now, seems to be produced by the presence of an asymmetric accumulation of the small particles (SP) around the large particles (LP) induced by the electric field.

The anomalous orientation is the only new electrokinetic phenomenon of bidispersed suspensions described up to now, but it has stimulated further investigations on electrokinetic measurements such as low-frequency dielectric dispersion (LFDD), where both the amplitude and characteristic frequencies are very sensitive to the properties of the medium, the particles, and their interfaces. For these reasons, interest in its

determination and its theoretical evaluation has increased during the past years [16–23].

This technique makes it possible to measure the $\alpha$-relaxation in the dielectric spectra caused by an electrolyte concentration gradient beyond the electrical double layer (EDL) [16]. The characteristic frequency of this relaxation is determined by the size of the particle. Hence, in principle, two different sizes in the suspension should result in two relaxation phenomena at two different characteristic frequencies associated with the LP and the SP, respectively. In spite of the fact that the theory predicts that both relaxations are simply added in the spectra and do not affect each other for sufficiently dilute suspensions, such as the majority of those studied in this work, we will show that it is experimentally observed that the $\alpha$-relaxation of the LP is accelerated and the amplitude decreases with the concentration of the SP.

## 2. Theoretical background

Colloidal particles (including their EDLs) in aqueous suspensions polarize when an electric field is applied. Due to the different time scales of the various phenomena that contribute to the induced dipoles, the dielectric constant exhibits some relaxation phenomena when the frequency of the ac field is increased. At a low frequency (on the order of $10^4$–$10^5$ rad/s), a first relaxation (known as $\alpha$-relaxation) occurs. This is a consequence of the concentration polarization effect: counterions undergoing tangential electromigration (if the field is applied from left to right, and the particle charge is negative, counterions—cations—will move to the right of the particle; see Fig. 1a) find co-ions brought by the field in such a way that both counterions and co-ions accumulate on the right and are depleted on the left. The characteristic time for the formation of this electrolyte concentration gradient is the diffusion time [16],

$$\tau_\alpha \approx \frac{(a + \kappa^{-1})^2}{D}, \tag{1}$$

where $a$ is the particle radius, $\kappa^{-1}$ is the thickness of the EDL, and $D$ is the diffusion coefficient of the ions. $\tau_\alpha$ is on the order of $10^{-4}$ s, so the characteristic $\alpha$-relaxation frequency, $\omega_\alpha \approx 10^4$ rad/s.

For sufficiently high field frequency, this accumulation cannot form and the diffusion currents ($\vec{j}_D^\pm$ in Fig. 1a) will be frozen. Still, there is time for counterions to accumulate on the left and co-ions on the right side of the particles, respectively, as shown in Fig. 1b. This polarization is basically due to the mismatch between particle and medium conductivities [24–26]. However, this contribution will eventually also disappear when the characteristic Maxwell–Wagner–O'Konski relaxation frequency, $\omega_{MWO}$, is reached. This frequency depends on the particle, $K_p$, and the medium, $K_m$, conductivities as follows,

$$\omega_{MWO} = \frac{(1-\phi)K_p + (2+\phi)K_m}{(1-\phi)\varepsilon_p\varepsilon_0 + (2+\phi)\varepsilon_m\varepsilon_0}, \tag{2}$$

where $\varepsilon_0$ is the vacuum permittivity, $\varepsilon_m$ and $\varepsilon_p$ are, respectively, the dielectric constants of the medium and the particle, and $\phi$
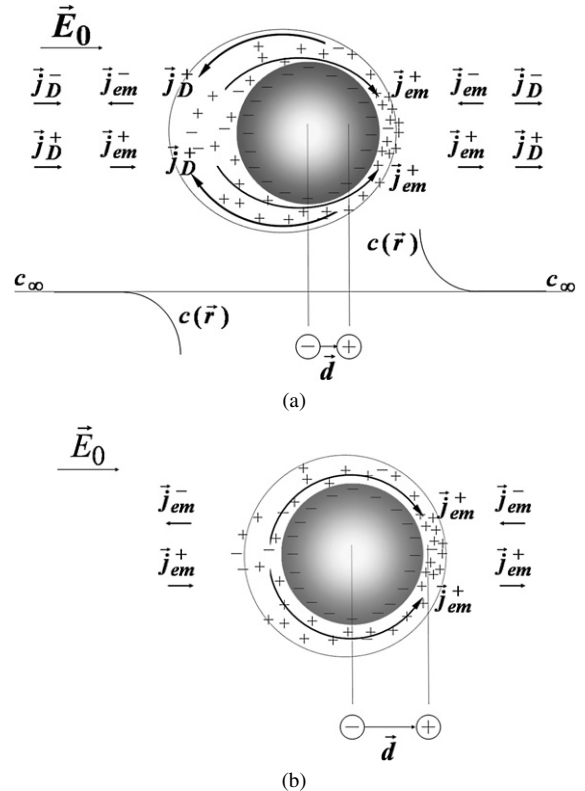


Fig. 1. Schematic representation of the fluxes of counterions (+) and co-ions (−) around a negatively charged colloidal particle in the presence of an electric field, $\vec{E}_0$. In (a) the concentration polarization (electrolyte concentration, $c(\vec{r})$, increased on the right and depleted on the left) brings about diffusion fluxes ($\vec{j}_D^\pm$) in addition to the electromigration ones ($\vec{j}_{em}^\pm$) due to the direct action of the field. In (b) the frequency is above the $\alpha$-relaxation and only electromigration fluxes remain.

is the volume fraction of solids. For the case of insulating particles with a charged atmosphere, the theory of the Maxwell–Wagner–O'Konski relaxation can still be used after replacing $K_p$ with an effective conductivity $K_p = 2K^\sigma/a$, where $K^\sigma$ is the so-called surface conductivity, which is a measure of the excess conduction parallel to the charged interface, produced by the excess of counterions in the electric double layer [27].

The value of this frequency is typically $10^8$ rad/s, i.e., about three orders of magnitude larger than $\omega_\alpha$.

Note that the processes described influence to a large extent the strength and direction of the dipole induced by the field. Thus, the ionic accumulation and depletion existing at low frequencies compress the EDL on the high-electrolyte-concentration side and expand it on the opposite side (Fig. 1a). As a consequence, there is a displacement between the centers of the EDL and particle charge distributions, thus modifying the induced dipole. In addition, the diffusion fluxes that oppose the electrolyte gradient ($\vec{j}_D^\pm$ in Fig. 1) redistribute the charge in the EDL, decreasing the induced dipole. On the other hand, these slow diffusion fluxes of counterions inside the EDL increase the displacement currents, leading to a huge value of the low-frequency permittivity of the suspension [16].

The $\alpha$-relaxation of dilute systems has been widely studied in the past [16–20,28,29]. Both in analytical and in numerical studies, the starting point is that the particles are well separated

and the dipolar field is not affected by the neighbor particles, and hence, the relative permittivity depends linearly on the particle concentration; that is,

$$\varepsilon'(\omega) = \varepsilon'_m + 3\phi\varepsilon'_m\left[ C_1(\omega) - \frac{K_m}{\omega\varepsilon_0\varepsilon_m} C_2(\omega) \right], \tag{3}$$

where $\omega$ is the angular frequency and $C_1$ and $C_2$ are the real and imaginary parts of the induced dipole coefficient related to the induced dipole by the expression

$$\vec{d} = 4\pi\varepsilon_0\varepsilon'_m a^3 [C_1 - iC_2]\vec{E}_0.$$

There are diverse approaches to the determination of the dipole coefficient. In fact, the models described above fail to explain the electrophoretic mobility and the conductivity measurements with the same parameters of the EDL. This obstacle is overcome if the stagnant-layer conductivity is taken into account [17,29–31]. Recall that the stagnant layer is a region adjacent to the solid surface in which the liquid is considered immobile. In the so-called standard electrokinetic model it is assumed that ions are also immobile, so that the conductivity of the layer is negligible. Speaking of stagnant-layer conductivity means assuming that, while the liquid is hydrodynamically stagnant, ions can move in response to an applied field, although perhaps with a mobility different from that in the bulk. This new ingredient improves the quantitative results but the main features remain the same as in the models without stagnant layer conductivity.

On the other hand, for concentrated colloidal suspensions, the linear relation between the dielectric increment and the particle concentration fails. Neighbor particles affect the hydrodynamic and electric fields around a given particle and hence modify the response of the latter to the external electric field. As a consequence, the dielectric increment differs from the predictions of a linear relation. In this case, the different approaches are based on the Kuwabara cell model [32], in which the whole suspension is replaced by an equivalent imaginary system consisting of a unique central particle of the same size surrounded by a finite shell of electrolyte. This model is combined with some appropriate electrostatic boundary conditions, of either Dirichlet or Neumann type [21,33].

In Fig. 2a is shown a typical spectrum [21] of the dielectric constant. There are two clearly observed relaxation processes

at $60 \times 10^3$ and $60 \times 10^6$ rad/s, respectively, and, accordingly, two absorption peaks in the spectrum of the imaginary part of the permittivity. Perhaps against intuition, it is found that the permittivity of the suspension depends in a nonlinear fashion on the volume fraction of solids even for unexpectedly low particle concentrations. For instance, in Fig. 2b, we show the dielectric increment for a suspension of particles for volume fractions ranging from 0.05 to 4%. The lack of linearity can be considered as a consequence of the existence of hydrodynamic and electric interactions between particles that disturb their individual contributions, thus reducing the positive influence on the permittivity of the dispersion.

## 3. Materials and methods

The suspensions are composed of large particles and small particles. As LP we used three kinds of negatively charged polystyrene latex spheres: L530, UCM190, and UCM177. In the case of L530, the charge comes from sulfonate groups on the surface, while the surface charges of UCM190 and UCM177 come from carboxylic groups. All these particles are essentially nonporous. The SP are negatively charged silica particles. The sizes and electrophoretic mobilities are detailed in Table 1. The pH of the suspensions was about 4.5, with little change upon addition of different volume fractions of either of the particles used.

The electrophoretic mobility measurements were performed in a Malvern ZetaSizer 2000 (Malvern Instrument, England) based on photon correlation spectroscopy. The electric permittivity of the suspensions was determined as a function of frequency (in the $3 \times 10^3$ to $6 \times 10^6$ rad/s range), by measuring the impedance of a thermostated conductivity cell with variable distance between the platinized platinum electrodes [34]. The applied field strengths were 91 mV/cm for the suspensions of UCM177 and 167 mV/cm for the samples L530 and UCM190. The logarithmic derivative procedure [35] was used to correct for electrode polarization and other stray capacitances. Briefly, this method is based on the analysis of the logarithmic derivative of the real part of the dielectric constant

$$\varepsilon''_D = -\frac{\pi}{2}\frac{\partial\varepsilon'(\omega)}{\partial\ln\omega}. \tag{4}$$

It can be shown that the contribution of electrode polarization behaves asymptotically as follows [35],

$$\varepsilon''(EP) = A\omega^{-1}, \tag{5}$$

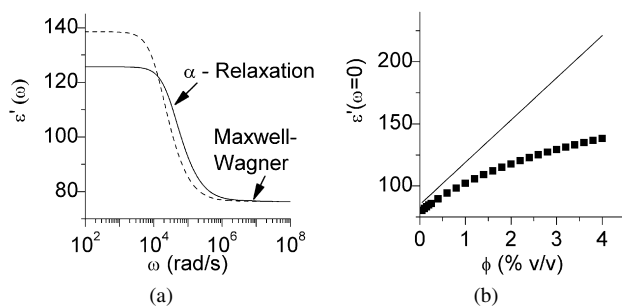$$\varepsilon''_D(EP) \propto L^{-1}\omega^{-3/2}, \tag{6}$$



Fig. 2. (a) Theoretical predictions of the model in [21] for the real part of relative permittivity of a suspension of 0.5 mM KCl and $\zeta = -100$ mV, $\phi = 0.02$, and $a = 200$ nm (—) and 400 nm (- - -). (b) (■) Theoretical predictions of the low-frequency dielectric constant of suspensions with 200-nm particles and different volume fractions ($\zeta = -100$ mV, 0.5 mM KCl). (—) Results obtained assuming a linear dependence on the volume fraction.

Table 1
Identification of the particles used, together with their radii and electrophoretic mobilities $u_e$ in 0.5 mM KCl solutions

| Particle | Radius (nm) | $u_e$ ($10^{-8}$ m$^2$ V$^{-1}$ s$^{-1}$) |
|---|---|---|
| L530 | 265 | −5.7 |
| UCM190 | 168 | −4.3 |
| UCM177 | 113 | −4.1 |
| A300 | 7.0 | −2.5 |

where $L$ is the distance between electrodes and $A$ is a constant. There are three advantages in using the logarithmic derivative instead of $\varepsilon''$: (i) Experimentally, the latter is calculated from conductivity measurements ($\varepsilon'' = (K - K(\omega = 0))/(\omega\varepsilon_0)$), and it remains undetermined at low frequency because of the noise; (ii) $\varepsilon''_D$(EP) decreases with the distance between electrodes, while $\varepsilon''$(EP) does not depend on it (compare Eqs. (5) and (6)); and (iii) the absorption peak of every dielectric relaxation is narrower in the spectra of $\varepsilon''_D$ than in the spectra of $\varepsilon''$. Hence, the electrode polarization contribution can be reduced if the electrodes are sufficiently separated. Furthermore, the high-frequency Maxwell–Wagner relaxation, usually a tiny contribution as compared to the $\alpha$-relaxation, can be observed as a separate peak in the spectrum of the logarithmic derivative, in contrast to that of $\varepsilon''$.

Fig. 3 shows an example of an experimental spectrum (full symbols in Fig. 3a) and its correction from electrode polarization by fitting the low-frequency part, where the electrode polarization is the main contribution (line in Fig. 3a) to Eq. (6). Note that the maxima in $\varepsilon''_D(\omega)$ are very well defined and allow reliable estimation of the $\alpha$-relaxation characteristic frequency or time. The dielectric increment of the suspension ($\delta\varepsilon'(\omega)$, full symbols in Fig. 3b) is then calculated from Eq. (4) by integrating the remaining $\varepsilon''_D$ data (open symbols in Fig. 3). According to Eq. (4), such integration would provide values of $\varepsilon'(\omega)$, except for an integration constant, and hence one is in fact obtaining a dielectric increment $\delta\varepsilon'(\omega) = \varepsilon'(\omega) - \varepsilon'(\infty)$ using this procedure. Finally, the $\delta\varepsilon'(\omega)$ data are fitted to the real part of the Havriliak–Negami relaxation function [36],

$$\delta\varepsilon'(\text{HN}) = \text{Re}\big\{\delta\varepsilon^*(\text{HN})\big\} = \text{Re}\left\{\frac{\Delta\varepsilon}{[1 + (i\omega\tau)^a]^b}\right\}, \qquad (7)$$

and this makes it possible to quantitatively estimate the amplitude of the relaxation by means of the $\Delta\varepsilon$ (equivalent to $\delta\varepsilon'(0)$) parameter.

All experiments were carried out at 25 °C.

## 4. Experimental results

Fig. 4 illustrates the goodness of the method used in two aspects. First, it shows that no relaxation is observed if a pure electrolyte solution is measured, as expected from the absence of any interfacial relaxation. Second, the figure demonstrates that the small A300 particles do not display any relaxation either, since the expected $\alpha$-relaxation frequency for these particles ($\approx 6 \times 10^6$ rad/s) is beyond our experimental limit. In contrast, one can clearly observe an absorption peak of UCM190 suspensions for frequencies around $20 \times 10^3$ rad/s, a typical value for particles around 300 nm in size (similar to that of UCM190).

Let us now consider how the permittivity of the suspensions of LP is influenced by the addition of SP (A300). Fig. 5 shows the results for both the logarithmic derivative of the permittivity $\varepsilon''_D(\omega)$ (Eq. (4)) and the real part of the dielectric increment $\delta\varepsilon'(\omega)$, when the LP is UCM190, for three ionic strengths and different A300 concentrations. Through simple visual inspection it is clear that (except for the lowest ionic strength tested) the addition of the nanoparticles both reduces the amplitude of the $\alpha$-relaxation and increases the relaxation frequencies. This is also true for L530 latex suspensions, as Fig. 6a demonstrates. In contrast, the UCM177 suspensions do not seem to be affected in their dielectric relaxation upon addition of A300.

A summary of the main features of the relaxation spectra, namely, $\Delta\varepsilon$ and the characteristic time, $\tau$ (Eq. (7)), for UCM190 and L530 is given in Figs. 7 and 8, respectively, as a function of the concentration of A300. Briefly, one can say that adding the A300 SP leads to a decrease in $\Delta\varepsilon$ (Fig. 7a). Note that the increase observed for the lowest ionic strength is most likely an artifact due to the fact that the small relaxation amplitude is hindered by the electrode polarization; hence, the uncertainty in this low ionic strength is too large to make any conclusion about the observed variations in the graph. The overall trends of both $\Delta\varepsilon$ and $\tau$ to decrease are confirmed by the L530 data in Fig. 8, where A300 concentrations up to 3.5% (v/v) have been included.

Note that according to Eq. (1), the characteristic time should decrease with ionic strength (since the thickness of the double layer $\kappa^{-1}$ decreases) and increase with the particle radius. However, in Fig. 7b, we observe an increase in $\tau$ with ionic strength, and the comparison between this figure and Fig. 8 suggests a lower characteristic time for the larger L530 particles. These are apparent effects, due to the unavoidable electrode polarization. Comparing Figs. 3 and 4, it is clear that in the case
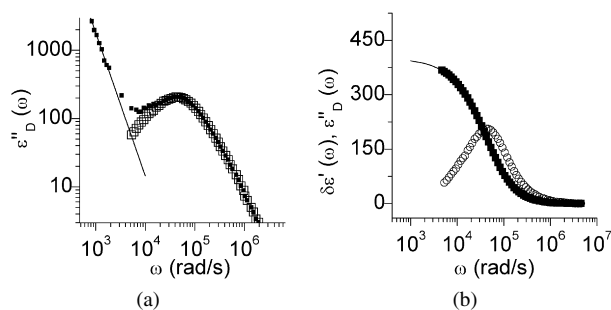


Fig. 3. (a) Logarithmic derivative of the dielectric constant of a 2% suspension of L530 in a 0.5 mM KCl solution. (■) Experimental results; (□) data corrected from the electrode polarization; (—) best fit of Eq. (6) to the low-frequency part of the spectra. (b) Dielectric increment (■) and logarithmic derivative of the dielectric constant (○) of the same suspension. (—) Best fit of the Havriliak–Negami function to the relative permittivity.
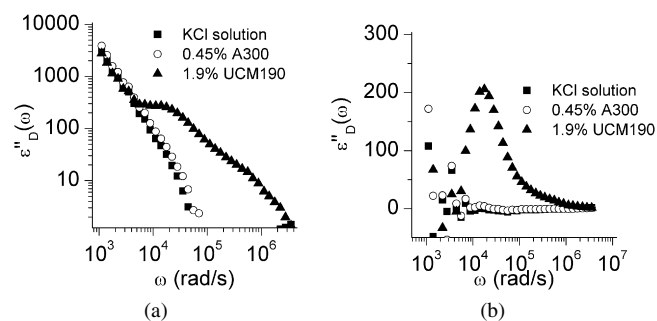


Fig. 4. Logarithmic derivative of the dielectric constant of a solution of 1 mM KCl (■), a suspension of A300 0.43% and 1 mM KCl (○), and UCM190 1.9% and 1 mM KCl (▲): (a) Without electrode polarization correction; (b) after electrode polarization correction.
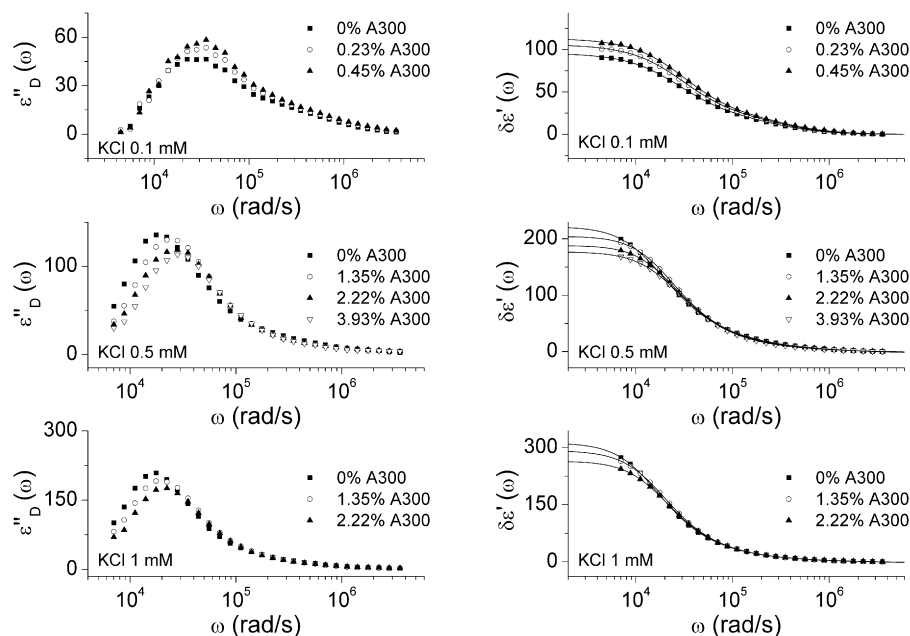
Fig. 5. Left: logarithmic derivative of the permittivity of UCM190 suspensions (1.9% volume fraction) for the KCl concentrations and different amounts of A300 nanoparticles added (indicated as % volume fraction). Right: dielectric increment of the same suspensions. Lines: best fits of the real part of $\varepsilon^*$(HN) (Eq. (7)).
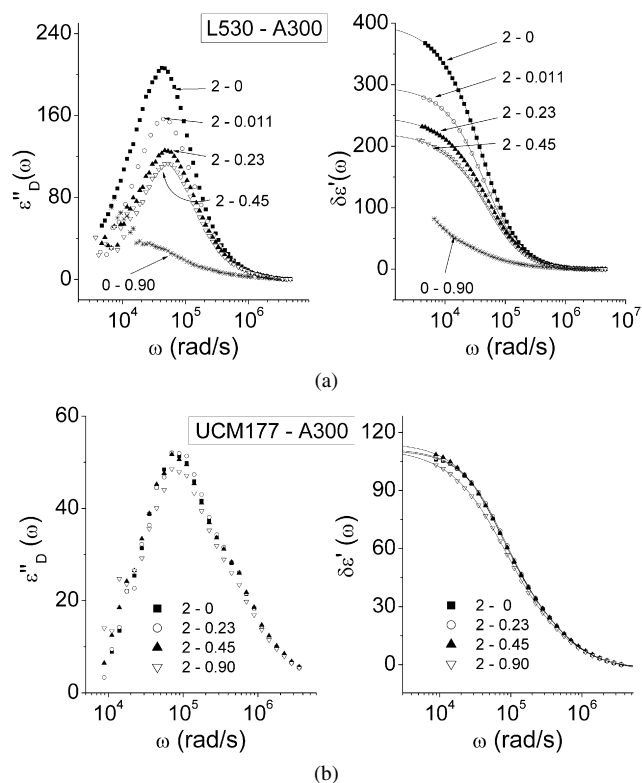


Fig. 6. Left: logarithmic derivative of the permittivity of L530 (a) and UCM177 (b) latex particles (2% volume fraction) in 0.5 mM KCl solutions. Right: dielectric increment of the same suspensions. The lines are the best fits of the real part of $\varepsilon^*$(HN) (Eq. (7)). The labels correspond to (LP concentration, %) − (A300 concentration, %).
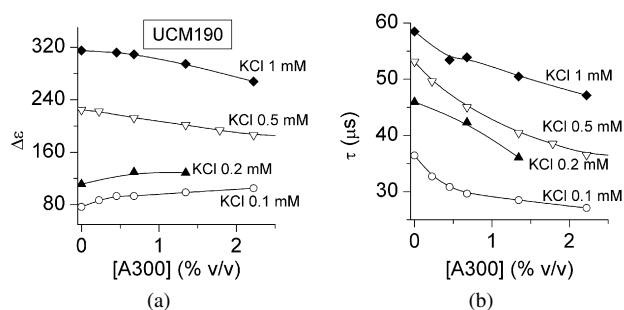
Fig. 7. Dielectric increment at zero frequency (a) and characteristic time (b) of the suspensions of UCM190 as a function of A300 concentration, for the indicated ionic strengths.
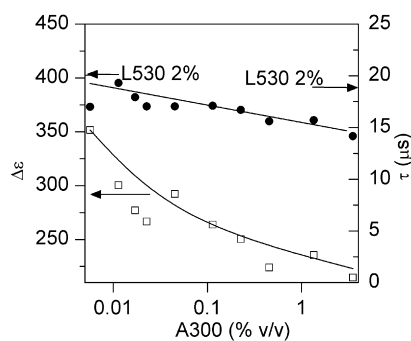
Fig. 8. Dielectric increment at zero frequency (□) and characteristic time (●) of suspensions of L530 as a function of A300 concentration. The arrows indicate the dielectric increment at zero frequency (left) and the characteristic time (right) for the suspensions of 2% L530 without added A300. KCl concentration 0.5 mM in all cases.

of UCM190 particles the absorption peak is partially masked by the electrode polarization decay, while these two processes are better separated in the case of L530. Hence, the characteristic frequency in the first case appears lower (the characteristic

time longer) than in the second case, even though the UCM190 particles are smaller. On the other hand, the electrode polarization increases with the conductivity of the suspension, hence, also the characteristic time.

Nevertheless, we may trust that for a given ionic strength, the electrode polarization will not be much affected by other experimental parameters, particularly, the solid contents. In fact, if we add A300, the conductivity of the sample should either increase or not vary at all. This would lead to either an increasing or a constant time, and we observe a decrease in $\tau$, as observed in Fig. 7b. Moreover, this behavior is observed in all samples without exception, so we believe that it is a real tendency rather than an artifact. This means that the effect of A300 concentration observed in Figs. 7b and 8 is an actual one, unlike the apparent increase in $\tau$ with ionic strength, which must be taken with caution.

## 5. Discussion

As previously mentioned, the overall behavior of a suspension in the presence of an external electric field is the sum of the individual responses of the particles and their ionic atmospheres, which in turn depend on the local particle concentration. Since the SP do not present any relaxation phenomena in the frequency range under study, their contribution to the permittivity is a constant and that does not affect the dielectric relaxation amplitude. In addition, considering that they are smaller than the LP, the concentration polarization dynamics is faster around the SP and will always be present during the formation of the concentration gradients around the LP, which are responsible for the $\alpha$-relaxation experimentally observed. Furthermore, according to Eq. (1), the possible aggregation or viscosity increase due to possible gel formation by A300 particles should lead to an increase of the characteristic time. It can also be argued that the observed behavior is the result of the overlapping of the electrical double layers of large and small particles. It is easy to prove that this is not the case in most of the suspensions considered: taking into account the double-layer thickness for the electrolyte concentration used, we can estimate the effective particle radius of the SP, and from this their effective volume fraction. This should be compared to the free volume left by the large particles. As a result, it is found that only for volume fractions of SP above 4.7% for 1 mM KCl, 2.5% for 0.5 mM KCl, and 0.9% for 0.2 mM KCl can we expect a significant double-layer overlap. Since most of our experiments were performed with lower volume fractions, a general explanation, valid also for such dilute systems, must be offered.

It is proposed that the concentration polarization around the SP located near the LP along the electric field direction (see Fig. 9a) partially counterbalances that around the LP and hence the amplitude of the $\alpha$-relaxation must decrease, in agreement with observations. On the other hand, the diffusion path length of the counterions decreases, and this leads to a shortening of the characteristic time of the dielectric relaxation (Fig. 9b), again in agreement with the experimental observation.

It is also worthwhile to compare the results for different salt concentrations and different LP. In Fig. 10 we show the relative decrement of $\Delta\varepsilon$ upon addition of A300 ($\Delta\varepsilon$(LP) is the dielectric increment of the suspensions without SP). In Fig. 10a we plot the results for two different salt concentrations and the latex UCM190, and it can be seen that the decrease in $\Delta\varepsilon$ with
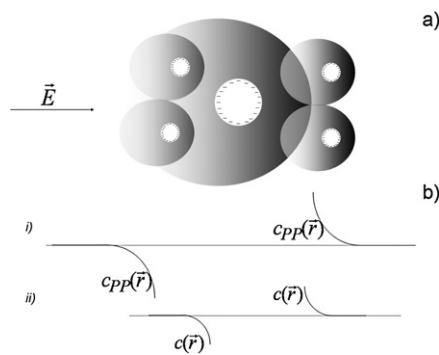


Fig. 9. (a) Schematic representation of one LP surrounded by SP. In the clouds, the darkest parts represent the highest electrolyte concentration. (b) The spatial distribution of concentration gradient for the LP alone (i) and the LP surrounded by SP (ii), respectively.
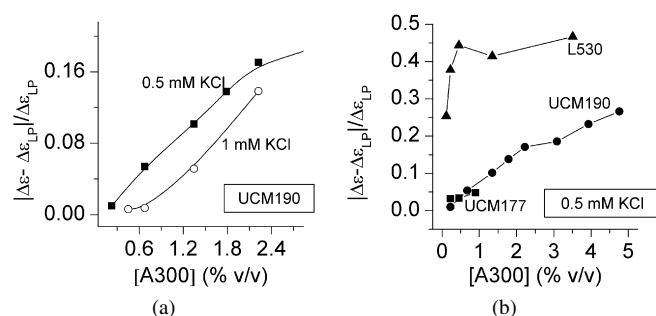


Fig. 10. Relative variation of the dielectric increment as a function of the volume fraction of A300. (a) Suspensions of UCM190 at 0.5 mM and 1 mM KCl. (b) The suspensions indicated with 0.5 mM KCl.

A300 concentration is more significant the smaller the ionic strength. This may arise from the fact that increasing the ionic strength compresses the double layer, shortening the counterion diffusion path, perhaps to distances smaller than those of maximum nanoparticle approach. Under such conditions, the effect of the small particles can be expected to be less noticeable, as observed.

Concerning the effect of the type of the large particles, let us mention that in [15] it was shown that under the action of the electric field, small particles accumulate on one side of the bigger particles, and this effect is magnified by the increase in the surface charge of the latter. Accordingly, the larger variation of the $\alpha$-relaxation amplitude in L530 can be explained by an increased (in comparison to the other LP) accumulation of SP due to the larger difference in their electrophoretic mobilities (see Table 1). This explanation agrees with the large differences observed in the case of L530 for a tiny addition of A300 (Fig. 10b) with respect to the L530 alone: if the accumulation mentioned should not occur, such a decrease in the suspension permittivity would only take place for a much higher A300 concentration. Only for such large numbers of small particles could one expect significant overlap between LP and SP polarization clouds. We conclude that the significant parameter is not the average concentration of A300 but its local concentration around the large particle, so that one could consider the bidisperse system under the action of an electric field as a nanoconcentrated system.

## 6. Conclusions

We have measured the low-frequency dielectric spectra of bidispersed systems formed by large particles and smaller particles, both negatively charged. We have observed a decrement of the amplitude and an acceleration of the $\alpha$-relaxation. These effects can be explained by an increase of the SP concentration around the LP, which reduces the electrolyte concentration gradient responsible for the comparatively high values of the low-frequency permittivity of colloidal suspensions.

## Acknowledgments

## References

[1] S. Fraden, A.J. Hurd, R.B. Meyer, Phys. Rev. Lett. 63 (1989) 2373.
[2] S.-R. Yeh, M. Seul, B.I. Shraiman, Nature 386 (1997) 57.
[3] D.G. Grier, Nature 424 (2003) 267.
[4] H. Isambert, A. Ajdari, J.-L. Viovy, J. Prost, Phys. Rev. Lett. 78 (1997) 971.
[5] P.P. Phule, J.M. Ginder, MRS Bull. August (1998) 19.
[6] H. Block, J.P. Kelly, J. Phys. D 21 (1988) 1661.
[7] A.P. Gast, C.K. Hall, W.B. Russel, J. Colloid Interface Sci. 96 (1983) 251.
[8] H.N.W. Lekkerkerker, W.C.K. Poon, P.N. Pusey, A. Stroobants, P.B. Warren, Europhys. Lett. 20 (1992) 559.
[9] G.A. Vliegenthart, H.N.W. Lekkerkerker, J. Chem. Phys. 111 (1999) 4153.
[10] M.A. Lauffer, J. Am. Chem. Soc. 61 (1939) 2412.
[11] U. Kraemer, H. Hoffmann, Macromolecules 24 (1991) 256.
[12] K.R. Foster, A.J. Osborn, M.S. Wolfe, J. Phys. Chem. 96 (1992) 5483.
[13] S.P. Stoylov, Adv. Colloid Interface Sci. 50 (1994) 51.
[14] S.P. Stoylov, E. Stoylova, J. Sturm, G. Weill, Biophys. Chem. 58 (1996) 157.
[15] F. Mantegazza, M. Caggioni, M.L. Jiménez, T. Bellini, Nature Phys. 1 (2005) 103.
[16] S.S. Dukhin, V.N. Shilov, Dielectric Phenomena and the Double Layer in Disperse Systems and Polyelectrolytes, Wiley, New York, 1974.
[17] F.J. Arroyo, F. Carrique, T. Bellini, A.V. Delgado, J. Colloid Interface Sci. 210 (1999) 194.
[18] L.A. Rosen, J.C. Baygents, D.A. Saville, J. Chem. Phys. 98 (1993) 4183.
[19] A.V. Delgado, F.J. Arroyo, F. González-Caballero, V.N. Shilov, Y.B. Borkovskaya, Colloids Surf. A 140 (1998) 139.
[20] J. Kijlstra, H.P. van Leeuwen, J. Lyklema, J. Chem. Soc. Faraday Trans. 88 (1992) 3441.
[21] F. Carrique, F.J. Arroyo, M.L. Jiménez, A.V. Delgado, J. Chem. Phys. 118 (2003) 1945.
[22] C. Grosse, J.J. López-García, J. Horno, J. Phys. Chem. B 108 (2004) 8397.
[23] A.V. Delgado, in: Interfacial Electrokinetics and Electrophoresis, in: Surfact. Sci. Ser., vol. 106, Dekker, New York, 2002.
[24] J.C. Maxwell, in: Electricity and Magnetism, vol. 1, Clarendon, Oxford, 1892.
[25] K.W. Wagner, Arch. Elektrotech. 2 (1914) 371.
[26] C.T. O'Konski, J. Phys. Chem. 64 (1960) 605.
[27] J. Lyklema, in: Fundamentals of Interface and Colloid Science, vol. II, Academic Press, London, 1995, pp. 431–437.
[28] E.H.B. DeLacey, L.R. White, J. Chem. Soc. Faraday Trans. II 77 (1981) 2007.
[29] C.S. Mangelsdorf, L.R. White, J. Chem. Soc. Faraday Trans. II 94 (1998) 2441.
[30] S.S. Dukhin, R. Zimmermann, C. Werner, Colloids Surf. A 195 (2001) 103.
[31] J. Lyklema, H.P. van Leeuwen, M. Minor, Adv. Colloid Interface Sci. 83 (1999) 33.
[32] S. Kuwabara, J. Phys. Soc. Jpn. 14 (1959) 527.
[33] V.N. Shilov, N.I. Zharkikh, Y.B. Borkovskaya, Colloid J. USSR 43 (1981) 434.
[34] M.C. Tirado, F.J. Arroyo, A.V. Delgado, C. Grosse, J. Colloid Interface Sci. 227 (2000) 141.
[35] M.L. Jiménez, F.J. Arroyo, J. van Turnhout, A.V. Delgado, J. Colloids Interface Sci. 249 (2002) 327.
[36] S. Havriliak, S. Negami, J. Polym. Sci. C 14 (1966) 99.